Cation-Exchange Kinetics of Sodium Complexes with Amide- and Ester-Substituted Crown Ethers in Homogeneous Solution

Yi Li, George Gokel, Jeanette Hernández, and Luis Echegoyen*

Contribution from the Department of Chemistry, University of Miami, Coral Gables, Florida 33124

Received September 20, 1993®

Abstract: The Na^+ complexes of 14 substituted aza-crown ethers, some containing amide and others containing ester functionalities in their side arms, were investigated by dynamic ^{23}Na NMR spectroscopy. Cation-exchange activation parameters and mechanisms between the complexes and the solvent were obtained in CD_3CN. The 18-C-6 derivatives exchange the cation via a primarily bimolecular or associative mechanism, while the 15-C-5 ligands prefer the unimolecular or dissociative pathway. The presence of the side arms containing donor groups is important in the bimolecular exchange process of the 18-C-6 systems, helping to effect the removal of the bound cation while a second one approaches the ligand from the opposite side of the molecule. The amide-substituted 15-C-5 complexes with Na^+ are very inert and exhibit characteristics similar to those of cryptates, with cation-exchange rates that are very slow, even at 70 °C. The observations suggest a very tight fit of Na^+ in the cavity provided by the 15-C-5 derivatives containing donor groups in the side arms. Although these are generally less thermodynamically stable than their 18-C-6 analogues, they are kinetically more stable.

Introduction

Two very common misconceptions in the field of crown ether–cation complexation are (1) that considerable knowledge has been accumulated concerning the cation-transporting abilities of crown ethers *across lipid bilayers* and (2) that the kinetics of cation exchange between the solvent and the ligand has a strong influence on the overall transport of cations *across bulk liquid membranes*. Nothing could be farther from the truth. With respect to point 1, only six reports have appeared which address directly the cation-transporting abilities of synthetic carriers across lipid bilayer environments.[1-6] One of the reasons for this, no doubt, has to do with the fact that lipid bilayer experiments are very difficult, while bulk liquid membrane methods are much easier to implement.[7] As a consequence, most of the literature related to the cation-transporting abilities of crown ethers has been developed using bulk liquid membranes.[7] A few examples have also appeared using solid-supported liquid membranes.[8] This brings us to the second misconception. When these liquid membrane models are used to study cation transport, the overall transport process is always controlled by diffusion across the membrane phase.[9] There is always equilibrium at the two membrane–water interfaces, and cation uptake or release by the "membrane"-bound ligand is never rate-determining.

Nevertheless, ligand–cation decomplexation kinetics can be very important when the work is done using lipid bilayers. For example, Riddell and co-workers have shown that Na^+ transport across large unilamellar vesicles (LUVs) mediated by several natural ionophores is always kinetically controlled by cation release from the complex.[10] So cation binding (and release) kinetics can be (and in many cases, is) rate-determining and thus very important, but only in lipid bilayer transport processes, not across bulk liquid membranes or solid-supported liquid membranes. It is thus important to measure the kinetics and to understand the mechanisms by which ligands, natural and synthetic, bind metal cations.

Although not as widespread as one might again imagine, there are several reports related to the kinetics and mechanisms of cation complexation and decomplexation using crown ethers.[11-14] At the time of writing of this paper, approximately 30 papers had been published related to kinetic studies of alkali metal–ionophore complexes using alkali metal NMR spectroscopy, most of these since the early 1980s. Notably important in this area is the seminal work of Schori et al. in 1971,[11] followed by the work of Popov and Dye,[12,13] and more recently that of Detellier et al.[14] These workers developed the methods to use NMR spectroscopy to obtain the kinetic parameters for these exchange reactions in homogeneous solution. They also extensively studied

* Abstract published in *Advance ACS Abstracts,* March 1, 1994.

(1) Kobuke, Y.; Yamamoto, J.-Y. *Bioorg. Chem.* **1990**, *18*, 283.
(2) Thomas, C.; Sauterey, C.; Castaing, M.; Gary-Bobo, C. M., Lehn, J.-M.; Plumere, P. *Biochem. Biophys. Res. Commun.* **1983**, *116*, 981.
(3) Castaing, M.; Morel, F.; Lehn, J.-M. *J. Membr. Biol.* **1986**, *89*, 251.
(4) Shinar, H.; Navon, G. *J. Am. Chem. Soc.* **1986**, *108*, 5005.
(5) Carmichael, V. E.; Dutton, P. J.; Fyles, T. M.; James, T. D.; Swan, J. A.; Zojaji, M. *J. Am. Chem. Soc.* **1989**, *111*, 767.
(6) Kragten, U. F.; Roks, M. F. M.; Nolte, R. J. M. *J. Chem. Soc., Chem. Commun.* **1985**, 1275.
(7) (a) Reusch, C. F.; Cussler, E. L. *AIChE J.* **1973**, 736. (b) Lamb, J. D.; Chistensen, J. J.; Izatt, S. R.; Bedke, K.; Astin, M. S.; Izatt, R. M. *J. Am. Chem. Soc.* **1980**, *102*, 3399. (c) Lamb, J. D.; Christensen, J. J.; Oscarson, J. L.; Nielsen, B. L.; Asay, B. W.; Izatt, R. M. *J. Am. Chem. Soc.* **1980**, *102*, 6820. (d) Kobuke, Y.; Hanji, K.; Horiguchi, K.; Asada, M.; Nakayama, Y.; Furukawa, J. *J. Am. Chem. Soc.* **1976**, *98*, 7414. (e) Kirch, M.; Lehn, J.-M. *Angew. Chem., Int. Ed. Engl.* **1975**, *14*, 555.
(8) (a) For a recent example, see: Nijenhuis, W. F.; Buitenhuis, E. G.; de Jong, F.; Sudhölter, E. J. R.; Reinhoudt, D. N. *J. Am. Chem. Soc.* **1991**, *113*, 7963. (b) Wienk, M. M.; Stalwijk, T. B.; Sudholter, E. J. R.; Reinhoudt, D. N. *J. Am. Chem. Soc.* **1990**, *112*, 797.
(9) (a) Behr, J.-P.; Kirch, M.; Lehn, J.-M. *J. Am. Chem. Soc.* **1985**, *107*, 241. (b) Fyles, T. *J. Membr. Sci.* **1985**, *24*, 229.
(10) (a) Riddell, F. G. *Chem. Br.* **1992**, 533. (b) Riddell, F. G.; Hayer, M. K. *Biochim. Biophys. Acta* **1985**, *817*, 313. (c) Riddell, F. G.; Arumugam, S.; Cox, B. G. *J. Chem. Soc., Chem. Commun.* **1987**, 1890. (d) Riddell, F. G.; Arumugam, S. *Biochim. Biophys. Acta* **1988**, *945*, 65. (e) Riddell, F. G.; Arumugam, S. *Biochim. Biophys. Acta* **1989**, *984*, 6. (f) Riddell, F. G.; Tompsett, S. J. *Biochim. Biophys. Acta* **1990**, *1024*, 193. (g) Riddell, F. G.; Arumugam, S.; Brophy, P. J.; Cox, B. G.; Payne, M. C. H.; Southon, T. E. *J. Am. Chem. Soc.* **1988**, *110*, 734.
(11) Schori, E.; Jagur-Grodzinski, J.; Luz, Z.; Shporer, M. *J. Am. Chem. Soc.* **1971**, *93*, 7133.
(12) (a) Dye, J. L.; Andrews, C. W.; Ceraso, J. M. *J. Phys. Chem.* **1975**, *79*, 3076. (b) Philips, R. C.; Khazaeli, S.; Dye, J. L. *J. Phys. Chem.* **1985**, *89*, 600. (c) Cahen, Y. M.; Dye, J. L.; Popov, A. I. *Inorg. Nucl. Chem. Lett.* **1974**, *10*, 899. (d) Dye, J. L. *Prog. Macrocycl. Chem.* **1979**, *1*, 63.
(13) (a) Lin, J. D.; and Popov, A. I. *J. Am. Chem. Soc.* **1981**, *103*, 3773. (b) Schmidt, E.; Popov. A. I. *J. Am. Chem. Soc.* **1983**, *105*, 1873. (c) Szczygiel, P.; Shamsipur, M.; Hallenga, K.; Popov, A. I. *J. Phys. Chem.* **1987**, *91*, 1252. (d) Strasser, B. O.; Hallenga, K.; Popov, A. I. *J. Am. Chem. Soc.* **1985**, *107*, 789. (e) Strasser, B. O.; Popov, A. I, *J. Am. Chem. Soc.* **1985**, *107*, 7921.
(14) (a) Graves, H. P.; Detellier, C. *J. Am. Chem. Soc.* **1988**, *110*, 6019. (b) Briere, K. M.; Detellier, C. *J. Phys. Chem.* **1987**, *91*, 6097. (c) Briere, K. M.; Detellier, C. *J. Phys. Chem.* **1992**, *96*, 2185. (d) Stover, H. D. H.; Detellier, C. *J. Phys. Chem.* **1989**, *93*, 3174.

0002-7863/94/1516-3087$04.50/0

the dissociative versus bimolecular nature of the mechanisms and explored the effects of concentration, cation, solvent, counteranion, and temperature on these exchange equilibria.[12-14] While these effects have been explored in considerable detail, the effect of ligand structure on the mechanisms has hardly been addressed.

Up until now, few reports have directly addressed the effects of ligand structure on the exchange mechanisms.[15,16] The dissociation of the dibenzo-24-C-8/Na^+ complex in nitromethane was found to proceed via the bimolecular pathway, *vide infra*, while 18-C-6/Na^+ followed a unimolecular pathway under the same experimental conditions. What seems to be missing most notably from the literature are similar studies involving a wider variety of crown ether systems. Little work has been done with crown ether systems beyond those with 15-C-5, 18-C-6, their benzo-substituted analogues, diaza-18-C-6, dithia-18-C-6, and dibenzo-24-C-8.[11-16] To our knowledge, no other cation–crown ether complexes have been systematically investigated and no homogeneous cation-exchange kinetics have ever been reported for substituted aza-crown ether systems.

In an effort to evaluate the importance of synthetic ionophores as potential antibiotic agents that mimic the action of natural ones in lipid bilayers, we present here the kinetic results for a complete series of amide- and ester-substituted and highly lipophilic crown ether–cation complexes. As part of their complete characterization, we report here their cation decomplexation kinetics in homogeneous acetonitrile solution. Many of these have been evaluated as Na^+ transporters in liposomes, and those results were reported separately.[17]

Description of the Model and the Equations

Although the model is the same, the nomenclatures used by Popov et al.[12,13] and by Detellier et al.[16,18] have small but significant differences. Thus we present here the complete set of equations used to analyze the ^{23}Na NMR data in the present work, which resemble more those of Popov et al. but follow the conventions of Detellier et al.[12-16,18]

It has been found that the complexation reactions of crown ethers (L) and their derivatives are usually diffusion-controlled,[19,20] and thus their values are not accessible by typical NMR experiments. It is usually from the much slower dissociation process, k_B in eq 1, that the relevant kinetic and mechanistic information is obtained. The rate for the complexation reaction,

$$M^+ + L \underset{k_B}{\overset{k_A}{\rightleftharpoons}} (M\text{-}L)^+ \qquad (1)$$

k_A in eq 1, may still be obtained if the value of the stability constant (K_s) is determined independently in the same solvent system along with k_B, since $K_s = k_A/k_B$. Equation 1 assumes a two-jump model for the exchange of the cation, where the two different sites correspond to the complex, $(M\text{-}L)^+$, and the other is the solvated cation, M^+. Equation 1 is meant to represent the very general situation of cation binding and decomplexation of any ligand L with a cation M^+ and not to imply any specific mechanism for the cation exchange, although as written it implies a process that can be identified directly with a unimolecular decomplexation mechanism, *vide infra*.

Two basic mechanisms have been proposed to account for the observed NMR results when cation exchange is present, as depicted in eq 1. These mechanisms were postulated very early in the original paper by Schori et al.[11] The first is referred to as the unimolecular dissociation or dissociative exchange pathway and is conveniently represented by eq 2. Notice that this equation

$$(M\text{-}L) \underset{k_1}{\overset{k_{-1}}{\rightleftharpoons}} M^+ + L \qquad (2)$$

is identical to eq 1, except that rate constant k_{-1} has been used instead of the rate k_B and k_1 instead of k_A. Whereas eq 1 was not meant to contain mechanistic implications and was to simply represent the general exchange of the cation between its solvated and its complexed states, eq 2 is meant to imply that the reaction occurs exactly as depicted. It is evident why the mechanism is referred to as dissociative since the complex simply dissociates to give the free (solvated) cation and the ligand. On the other hand, the bimolecular cation-interchange mechanism, also known as the associative exchange mechanism, involves a second cation (M^{*+}) as shown in eq 3. The transition state for the latter

$$M^{*+} + (M\text{-}L)^+ \overset{k_2}{\rightleftharpoons} M^+ + (M^*\text{-}L)^+ \qquad (3)$$

mechanism involves a complex where two cations are partially bound simultaneously. The relative contributions of these two mechanisms to the observed processes can be conveniently obtained using variable concentrations and alkali metal NMR spectroscopy.[13b,18,21]

Without presenting the detailed derivation of the equations, suffice it to say that the average lifetime of the solvated Na^+, defined as τ_A, if assumed to be affected by the occurrence of reactions 2 and 3, is given by eq 4. On the other hand, the average

$$\frac{1}{\tau_A[M^+]_{complex}} = \frac{k_{-1}}{[M^+]_{free}} + k_2 \qquad (4)$$

lifetime between the two Na^+ exchange sites (A and B, where B represents the complex) could be defined as τ. Since $1/\tau = 1/\tau_A + 1/\tau_B$, then the final equation that is derived is very similar to eq 4, but it contains τ instead of τ_A and $[M^+]_{total}$ instead of $[M^+]_{complex}$, see eq 5. Since it was possible in most cases to detect

$$\frac{1}{\tau[M^+]_{total}} = \frac{k_{-1}}{[M^+]_{free}} + k_2 \qquad (5)$$

both Na^+_{free} and $Na^+_{complex}$ resonances simultaneously, *vide infra*, the kinetics were measured in the slow exchange regime.

In the slow exchange regime, the rate constant is conveniently calculated from the measured line width, since the Bloch equations simplify to eq 6 under these conditions.[22] W and W_0 in eq 6 refer

$$k = \Pi(W - W_0) \qquad (6)$$

to the line widths at half-height for a Na^+ signal in the presence and absence of exchange, respectively. In the present study, the Na^+_{free} resonance was used for the calculations.

It is fairly easy to determine the relative contributions of the two competing mechanisms by simply plotting $1/\tau_A[M^+]_{complex}$ vs $1/[M^+]_{free}$ or $1/\tau[M^+]_{total}$ vs $1/[M^+]_{free}$. From the slopes and intercepts it is easy to obtain the values of the exchange rate constants, k_{-1} and k_2, and thus to determine the relative importance of their respective contributions.

(15) (a) Delville, A.; Stover, H. D. H.; Detellier, C. *J. Am. Chem. Soc.* **1985**, *107*, 4172. (b) Delville, A.; Stover, H. D. H.; Detellier, C. J. *J. Am. Chem. Soc.* **1987**, *109*, 7293.
(16) Shamsipur, M.; Popov, A. I. *J. Phys. Chem.* **1988**, *92*, 147.
(17) Xie, Q.; Li, Y.; Gokel, G.; Hernández, J.; Echegoyen, L. *J. Am. Chem. Soc.* **1994**, *116*, 690.
(18) Detellier, C.; Graves, H. P.; Briere, K. M. *Isotopes in the Physical and Biomedical Science*; Elsevier Science Publishers: Amsterdam, 1991; Chapter 4.
(19) Bouquant, J.; Delville, A.; Grandjean, J.; Laszlo, P. *J. Am. Chem. Soc.* **1982**, *104*, 686.
(20) Chock, P. B. *Proc. Nat. Acad. Sci. U.S.A.* **1979**, *69*, 1939.
(21) Detellier, C. In *Modern NMR Techniques and Their Application in Chemistry*; Popov, A. I.; Hallenga, K., Eds.; Marcel Dekker, Inc.: New York, 1990; Chapter 9.
(22) Sandstrom, J. *Dynamic NMR Spectroscopy*; Academic Press Publishers: New York, 1982.

One fairly easy way to qualitatively determine the relative importance of these two mechanisms is to do a variable concentration experiment.[16,23] Since the relative ratio of $[Na^+]_{total}$ to L was always kept constant at a value of 2, *vide infra*, the ratio $[Na^+]_{total}/[Na^+]_{free}$ was also always equal to 2, since the stability constants are all relatively high.[24] Rewriting eq 5 as eq 7, it is

$$\frac{1}{\tau} = k_{-1}\frac{[M^+]_{total}}{[M^+]_{free}} + k_2[M^+]_{total} \qquad (7)$$

easy to see that a pronounced effect on τ is expected from changing $[M^+]_{total}$ if there is a significant contribution from k_2. On the other hand, no spectral changes are anticipated if k_{-1} is dominant. It is thus easy to check the relative importance of these mechanisms by simply diluting a sample and recording the NMR spectra at both concentrations. It is possible sometimes to change from a spectrum clearly exhibiting two separate Na^+ resonances at low total concentrations to a "coalesced" spectrum by simply increasing the total concentration, *vide infra*.

In addition to variable concentration studies designed to unravel mechanistic details, variable temperature studies were also conducted to determine the values of the activation parameters for the dissociation reactions.

Results and Discussion

The general structures of the compounds studied are presented below. In order to simplify the nomenclature while keeping

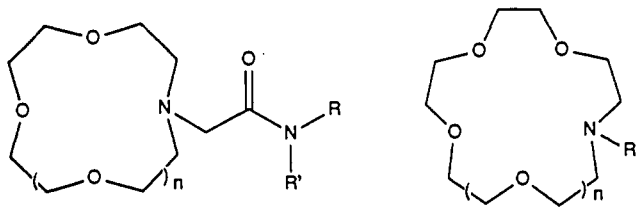

relatively informative names for the compounds used in this study and to avoid using numerals to identify them, the following scheme was adopted.[24] The symbol (00N) was used to represent an aza-lariat ether having 00 atoms in the macroring. Side arms attached to the macroring nitrogen are explicitly written following the ring identifier. Only one diaza compound was studied here, and it is represented by $(N18N)[CH_2\text{-}CO\text{-}N(C_5H_{11})_2]_2$, indicating that it is a 1,10-diaza-18-C-6, and each macroring nitrogen is directly substituted with one dialkyl amide functionality. A total of 16 structures were investigated, see list in Table 1. In addition to the secondary and tertiary amide-substituted and ester-substituted crown ether compounds, two alkyl-substituted compounds were included for comparison along with unsubstituted 15-C-5 and 18-C-6.

Since kinetic information was desired for such a large number of compounds, it was somewhat unfeasible to do a detailed total line shape fitting for all compounds close to the coalescence temperature. Therefore, an effort was made to directly measure spectra below it, in the slow exchange regime. In such cases the line width of the Na^+_{free} resonance was used for all of the calculations. For those where the chemical shifts between Na^+_{free} and $Na^+_{complexed}$ were too small to allow significant measurements, as in most 18-C-6 derivative complexes, only the coalescence temperature and the line width at that temperature were determined. For these, the activation energies at the coalescence temperatures were calculated for comparison. It was felt that comparisons between these values would be meaningful, even if a complete line shape analysis was not executed.

(23) Lochhart, J. C.; McDonnell, M. B.; Clegg, W.; Hill, M. N. S.; Todd, M. *J. Chem. Soc., Dalton Trans.* **1989**, 203.
(24) Hernández, J. C.; Trafton, J. E.; Gokel, G. W. *Tetrahedron Lett.* **1991**, 6269.

Table 1. ^{23}Na NMR Chemical Shifts and Line Widths of the Crown Ether Derivative/Na^+ Complexes Measured at a 2:1 Na^+/Ligand Ratio in CD_3CN at –40 °C

compound	chemical shift (ppm) δ_c	chemical shift (ppm) δ_f	line width (Hz) W_c	line width (Hz) W_f
NaBPh4		–7.6		20
$\langle 12N\rangle CH_2\text{-}CO\text{-}N(C_5H_{11})_2$	–1.7	–7.6	357	82
$\langle 15N\rangle CH_2\text{-}CO\text{-}N(C_5H_{11})_2$	–1.0	–7.7	541	34
$\langle 15N\rangle CH_2\text{-}CO\text{-}N(C_{10}H_{21})_2$	–0.8	–7.5	*a*	85
$\langle 15N\rangle CH_2\text{-}CO\text{-}NHC_5H_{11}$	–1.1	–7.7	387	43
$\langle 15N\rangle CH_2\text{-}CO\text{-}NHC_{10}H_{21}$	–1.0	–7.8	440	26
$\langle 15N\rangle CH_2\text{-}CO\text{-}OC_{10}H_{21}$	–2.5	–7.8	287	26
$\langle 15N\rangle C_4H_9$	–5.2	–7.7	124	34
15-C-5	–6.5	–7.7	*a*	*a*
18-C-6	–15.7[b]	–7.7	194	77
$\langle 18N\rangle C_3H_6CHCH_2$	–9.4[c]	–7.8	*a*	32
$(N18N)[CH_2\text{-}CO\text{-}N(C_5H_{11})_2]_2$	–1.3	–7.7	589	49
$\langle 18N\rangle CH_2\text{-}CO\text{-}N(C_5H_{11})_2$	–7.2[c]	–7.8	*a*	50
$\langle 18N\rangle CH_2\text{-}CO\text{-}N(C_{10}H_{21})_2$	–7.2[c]	–7.8	*a*	53
$\langle 18N\rangle CH_2\text{-}CO\text{-}NHC_{18}H_{37}$	–8.1[c]	–7.8	*a*	31
$\langle 18N\rangle CH_2\text{-}CO\text{-}OC_{10}H_{21}$	–9.2[c]	–7.8	320[c]	26

[a] The line width cannot be measured because of signal overlap. [b] Our data are in good agreement with literature results.[13a,14a] [c] Estimated value.

One immediate concern was the available temperature range in CD_3CN and the feasibility of "freezing" all of the cation-exchange equilibria. Of even more concern was the need to go down in temperature in order to make several measurements of the line widths of the Na^+_{free} resonances, sufficiently separated from those of $Na^+_{complexed}$. As it turns out and somewhat surprisingly, this concern was not a problem for many of the systems studied.

Our expectation was that many of the alkali cation complexes of these ligands would be in the fast exchange region in CD_3CN, especially at room temperature, and that only one averaged resonance would be observed in these cases. We were surprised to see that two well-resolved resonances were clearly obtained by ^{23}Na NMR spectroscopy for many of these complexes in CD_3CN in the presence of an excess of $NaBPh_4$. This was true for the Na^+ complexes of $\langle 15N\rangle CH_2\text{-}CO\text{-}N(C_5H_{11})_2$, $\langle 15N\rangle CH_2\text{-}CO\text{-}N(C_{10}H_{21})_2$, $\langle 15N\rangle CH_2\text{-}CO\text{-}NHC_5H_{11}$, $\langle 15N\rangle CH_2\text{-}CO\text{-}NHC_{10}H_{21}$, and $\langle 15N\rangle CH_2\text{-}CO\text{-}OC_{10}H_{21}$ at 21 °C. At –40 °C, most Na^+ complexes in this study exhibited two resolved resonances for Na^+_{free} and $Na^+_{complexed}$, see Table 1 for their chemical shifts and line widths. It was thus possible to freeze the equilibria in these cases and to measure W for Na^+_{free} to obtain τ_A. Figure 1 shows typical examples of ^{23}Na NMR spectra of the 15-crown derivative/Na^+ complexes at a 2:1 Na^+/ligand ratio measured at 21 °C and the 12- and 18-crown derivative/Na^+ complexes at –40 °C. It is evident that for the 15-crown/Na^+ complexes the Na^+ cation exchange is in the slow exchange regime even at room temperature. However, this was not the case for the 12- and some of the 18-crown/Na^+ complexes, but these were frozen at –40 °C (d–f in Figure 1). Note also the significant chemical shift difference between the complexed Na^+ resonance of 18-C-6/Na^+ and that of $(N18N)[CH_2\text{-}CO\text{-}N(C_5H_{11})_2]_2/Na^+$, *vide infra*.

The choice of CD_3CN as the best solvent for the present studies was not fortuitous. Figure 2 shows the ^{23}Na NMR spectra of $\langle 15N\rangle CH_2\text{-}CO\text{-}N(C_5H_{11})_2/Na^+$ in four different solvents, ranging from methanol to acetonitrile. As expected, the rate of exchange followed the same trend as the Gutman donicity numbers of these solvents, with the values decreasing in the order MeOH > DMSO > acetone > CD_3CN.[25] Therefore, CD_3CN was chosen in order to enhance the chances of observing two separate Na^+ resonances for the complexes in equilibrium with the solvated cation.

(25) Gutmann, V.; Wychera, E. *Inorg. Nucl. Chem. Lett.* **1966**, *2*, 257.

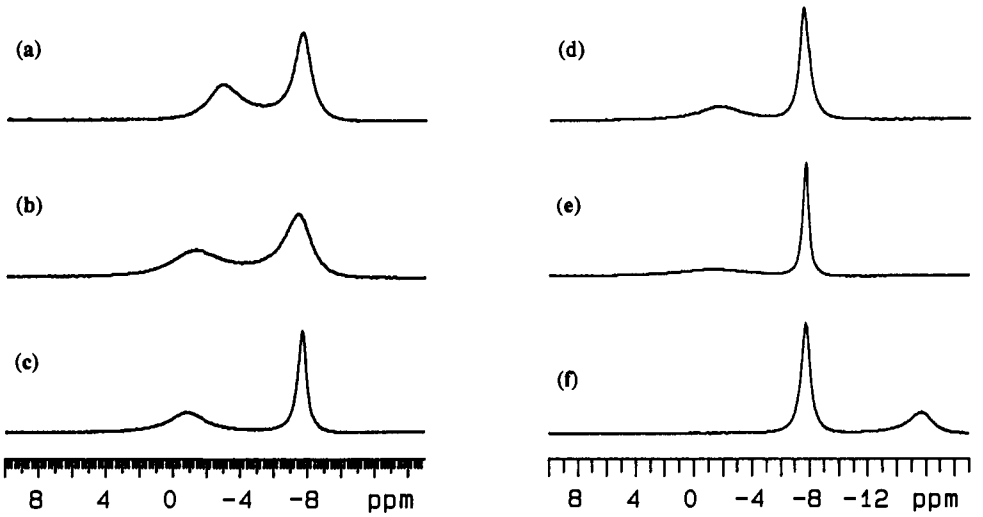

Figure 1. ^{23}Na NMR spectra of $\langle 15N\rangle CH_2$-CO-$OC_{10}H_{21}/Na^+$ (a), $\langle 15N\rangle CH_2$-CO-NHC_5H_{11}/Na^+ (b), and $\langle 15N\rangle CH_2$-CO-$N(C_5H_{11})_2/Na^+$ (c) measured in CD_3CN with a 2:1 Na^+/ligand ratio at room temperature and of $\langle 12N\rangle CH_2$-CO-$N(C_5H_{11})_2/Na^+$ (d), $\langle N18N\rangle[CH_2$-CO-$N(C_5H_{11})_2]_2/Na^+$ (e), and 18-C-6/Na^+ (f) at −40 °C.

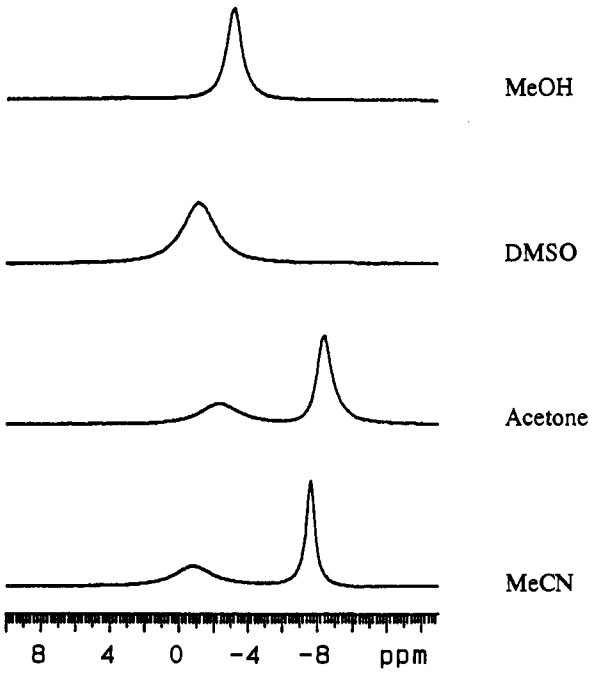

Figure 2. ^{23}Na NMR spectra of $\langle 15N\rangle CH_2$-CO-$N(C_5H_{11})_2/Na^+$ complex in different solvents with a Na^+/ligand ratio of 2:1.

Structural Implications. Before a detailed analysis of the kinetic results is presented, the chemical shifts and the line widths reported in Table 1, along with some variable temperature observations, will be used to infer some general structural characteristics about these complexes in solution. The first is side-arm participation in the cation-binding process.

Note that the line widths of the complexed ^{23}Na resonances for the ligands that contain donor groups in the side arm(s) are always larger than those of the corresponding complexes with the model systems. For example, the lowest measurable line width in the 15-C-5 series of complexes is exhibited by the model compound $\langle 15N\rangle C_4H_9$ at 124 Hz. All other 15-C-5 complexes had considerably larger line widths, see Table 1. The same observation holds true for the few cases that were measurable in the 18-C-6 series. The lowest line width is exhibited by the complex with 18-C-6 itself at 194 Hz. Such an observation reflects the fact that these complexes containing donor groups in the side arms generate electrical field gradients around the Na^+, thus decreasing the overall symmetry and giving rise to broader resonances. This is direct evidence that the sidearms participate in the overall binding process to some degree.

Further evidence of this can be found in the correlation that exists between the basicity of the side-arm group and the downfield shifts of the complexed ^{23}Na resonances. At room temperature the following order was found for the 15-C-5 series: $\langle 15N\rangle$-CH_2-CO-$N(C_5H_{11})_2/Na^+ \sim \langle 15N\rangle CH_2$-CO-$N(C_{10}H_{21})_2/Na^+ > \langle 15N\rangle CH_2$-CO-$NHC_5H_{11}/Na^+ \sim \langle 15N\rangle CH_2$-CO-NH-$C_{10}H_{21}/Na^+ > \langle 15N\rangle CH_2$-CO-$OC_{10}H_{21}/Na^+ > \langle 15N\rangle C_4H_9/Na^+$. The order observed for the 18-C-6 series was identical. The 18-C-6 diamide-substituted ligand showed the most downfield-shifted resonance, in agreement with the observed trend, since the effect of the two amide substituents is expected to be additive. It is thus evident that the donor side arms are involved in the cation-binding process in all of these ligands.

Another interesting observation that can be made directly from the data in Table 1 is that all of the 15-C-5 and the 12-C-4 complexes experience paramagnetically shifted signals, while some 18-C-6 complexes exhibit diamagnetic shifts relative to the solvated cation resonance. Some of the 18-C-6 complexes have ^{23}Na resonances that are very close to that of the solvated Na^+, but only one 18-C-6 derivative has a pronounced paramagnetically shifted resonance, $\langle N18N\rangle[CH_2$-CO-$N(C_5H_{11})_2]_2$. A similar trend was observed by Lehn et al. in their kinetic study of cryptand/Na^+ complexes.[26] The chemical shifts of the complexed ^{23}Na resonances for [2.1.1]/Na^+, [2.2.1]/Na^+, and [2.2.2]/Na^+ were 11.15, −4.25, and −11.40 ppm, respectively. A linear relationship has been proposed[27] between the quadrupole coupling constant (χ_{Na}) and the paramagnetic shielding term which dominates the ^{23}Na chemical shifts. Such a correlation was observed experimentally between χ_{Na} and the chemical shift (δ).[26] Since χ is proportional to the electric field gradients, the different chemical shift trends exhibited by the 18-C-6 derivative complexes when compared to those of the 15-C-5 and 12-C-4 analogues are indicative of a less symmetric coordination sphere in the latter. The exception in the trend of the 18-C-6 series was observed for $\langle N18N\rangle[CH_2$-CO-$N(C_5H_{11})_2]_2$. In this case, there are very strong interactions between the bound cation and the two side-arm amide carbonyls. Since the ^{23}Na line width observed for this complex at −40 °C is very large, 589 Hz, it is believed that the interaction with the two carbonyls occurs from the same side of the macroring, in a syn conformation. This introduces a more

(26) Kintzinger, J. P.; Lehn, J.-M. *J. Am. Chem. Soc.* **1974**, *96*, 3313.
(27) Deverell, C. *Mol. Phys.* **1969**, *16*, 491.
(28) White, B. D.; Mallen, J.; Arnold, K. A.; Fronczek, F. R.; Gandour, R. D.; Gehring, L. M. B.; Gokel, G. W. *J. Org. Chem.* **1989**, *54*, 937.
(29) Cahen, Y. M.; Dye, J. L.; Popov, A. I. *J. Phys. Chem.* **1975**, *79*, 1292.

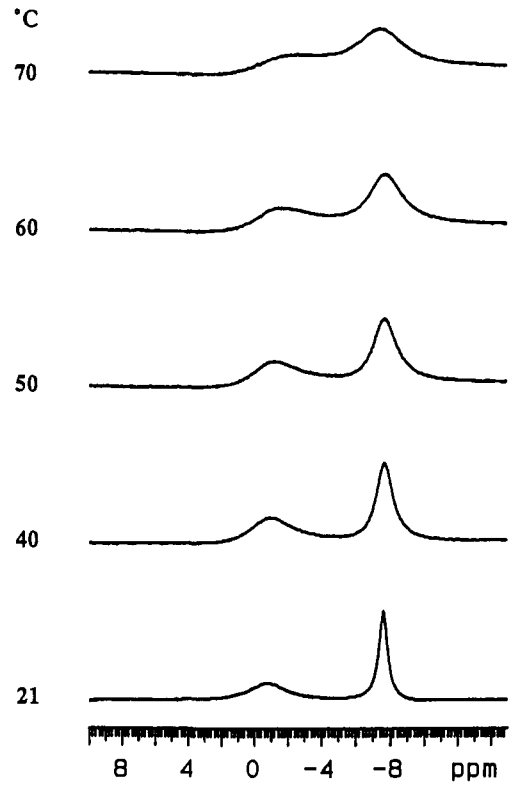

Figure 3. ^{23}Na NMR spectra of $\langle 15N\rangle CH_2$-CO-$N(C_5H_{11})_2/Na^+$ complex at various temperatures.

pronounced unsymmetrical environment than if the interaction occurred in an anti conformation. Although the side arms are bulky and a syn conformation might seem unfavorable, other diaza-18-C-6/Na^+ complexes containing fairly bulky substituents have been shown to adopt such a conformation by X-ray crystallography.[28] In that report, the two side arms were (Gly-Gly-OMe), yet the syn conformation was adopted.[28]

In agreement with all of these observations, it is interesting to note that only two of the complexes studied did not exhibit coalescence of the Na^+ resonances at the highest available temperatures in CD_3CN, ~70 °C. Both of these complexes contained 15-C-5 rings. They were $\langle 15N\rangle CH_2$-CO-$N(C_5H_{11})_2/Na^+$ and $\langle 15N\rangle CH_2$-CO-$N(C_{10}H_{21})_2/Na^+$. Figure 3 shows the spectra for $\langle 15N\rangle CH_2$-CO-$N(C_5H_{11})_2/2Na^+$ between 21 °C and 70 °C, clearly showing that the two resonances remained resolved at the highest available temperature. This behavior is consistent with the assertion made above that the 15-C-5 derivatives seem to exhibit a better "fit" with the cation and is somewhat reminiscent of that exhibited by the cryptates.[29] These two ligands seem to be the most efficient of all of those studied at isolating the bound cation from exposure to the solvent. This relatively pronounced kinetic inaccessibility of the bound cation to the solvent molecules is indicative of the formation of inclusive-like and very stable complexes.

Determination of the Predominant Cation-Exchange Mechanisms Using Variable Concentration Experiments. Nine complexes were selected for the variable concentration studies, which represented all types of structures available: $\langle 12N\rangle CH_2$-CO-$N(C_5H_{11})_2$, $\langle 15N\rangle CH_2$-CO-$N(C_5H_{11})_2$, $\langle 15N\rangle CH_2$-CO-NH-C_5H_{11}, $\langle 15N\rangle CH_2$-CO-$OC_{10}H_{21}$, 15-C-5, $\langle 18N\rangle CH_2$-CO-$N(C_5H_{11})_2$, $\langle 18N\rangle CH_2$-CO-$OC_{10}H_{21}$, $\langle N18N\rangle[CH_2$-CO-N-$(CC_5H_{11})_2]_2$, and 18-C-6. At least three different total Na^+ concentrations were studied while the $[NaBPh_4]/[ligand]$ ratio was kept constant at a value of 2. The actual total Na^+ concentrations used ranged between 0.5 and 10 mM.

Representative spectra are shown in Figures 4 and 5, which clearly manifest the pronounced differences in the behavior of the 15-C-5 series when compared to that of the 18-C-6 series. Notice that all of the 15-C-5 complexes show either a very small spectral effect or no effect at all upon dilution, Figure 4. As implied by eq 7, this indicates that a predominantly unimolecular (dissociative) exchange mechanism controls the exchange of Na^+ between the complex and the solvent in these cases. Except for the behavior of 18-C-6, all other 18-C-6 derivative complexes exhibited pronounced spectral changes upon dilution, indicating a predominance of the bimolecular exchange mechanism in these cases. Notice from Figure 5 that in some cases it was even possible to go from a "concentration coalesced" signal to a time-resolved spectrum simply by diluting the sample (see the $\langle 18N\rangle CH_2$-CO-$OC_{10}H_{21}/Na^+$ and $\langle 12N\rangle CH_2$-CO-$N(C_5H_{11})_2/Na^+$ cases).

Using eq 6, the values of k were determined by directly measuring W for the solvated Na^+ resonance, but only in those cases exhibiting two base-line resolved signals at room temperature, 21 °C. The values of the unimolecular and bimolecular rate constants for the cation-exchange reaction were determined using eq 4 after appropriate construction of the $1/\tau_A[Na^+]_{complex}$ vs $1/[Na^+]_{free}$ plots. Representative plots are presented together in Figure 6 for the Na^+ complexes of $\langle 15N\rangle CH_2$-CO-$OC_{10}H_{21}$, $\langle 15N\rangle CH_2$-CO-NHC_5H_{11}, $\langle 15N\rangle CH_2$-CO-$N(C_5H_{11})_2$, and $\langle N18N\rangle[CH_2$-CO-$N(C_5H_{11})_2]_2$. Obviously, the unimolecular mechanism predominates for the first two ligands since the slopes are substantial while their intercepts are almost zero. On the other hand, the bimolecular mechanism predominates in the case of $\langle N18N\rangle[CH_2$-CO-$N(C_5H_{11})_2]_2$. Interestingly, $\langle 15N\rangle CH_2$-CO-$N(C_5H_{11})_2/Na^+$ does not exchange well by either one of these mechanisms. This is not surprising in view of the fact that it was not possible to reach the coalescence temperature even at 70 °C, *vide supra*.

It was only possible to obtain kinetic parameters for five of the nine ligands investigated. The values of k_{-1} and k_2 for these are presented in Table 2, along with their corresponding $\Delta G^{\ddagger}$ values calculated from the Eyring equation. The reasons why it was not possible to obtain the complete kinetic profile of all of these ligands varied for the different complexes. In the cases of $\langle 18N\rangle CH_2$-CO-$N(C_5H_{11})_2/Na^+$ and $\langle 18N\rangle CH_2$-CO-$OC_{10}H_{21}/Na^+$, the coalescence concentrations are too low to afford enough data for the calculations. However, based on the results from the dilution experiments (see Figure 5), it is reasonable to assume that the bimolecular mechanism is predominant for these two complexes. In the case of the parent 18-C-6/Na^+ and 15-C-5/Na^+ complexes, it was not possible to use eq 6, since the exchange is in the intermediate and fast regimes, respectively, not in the slow regime. However, these systems have been previously studied by Detellier et al. in several solvents including CH_3CN.[18,30] The entry for

Table 2. Kinetic Parameters for Unimolecular and Bimolecular Mechanisms Measured by ^{23}Na NMR in CD_3CN[a]

compound	$\Delta G^{\ddagger}_{21} \cdot c^{bi}$ (kcal/mol)	$\Delta G^{\ddagger}_{21} \cdot c^{uni}$ (kcal/mol)	k_2 (s^{-1} M^{-1})	k_{-1} (s^{-1})
$\langle 12N\rangle CH_2$-CO-$N(C_5H_{11})_2$	9.6(0.1)	14.09(0.03)	$4.7(0.8) \times 10^5$	205(9)
$\langle 15N\rangle CH_2$-CO-$N(C_5H_{11})_2$	11.4(0.1)	14.98(0.01)	$2.0(0.2) \times 10^4$	45(1)
$\langle 15N\rangle CH_2$-CO-NHC_5H_{11}	11.4(0.2)	13.53(0.04)	$2.2(0.9) \times 10^4$	536(4)
$\langle 15N\rangle CH_2$-CO-$OC_{10}H_{21}$	13.7(1.1)	13.74(0.01)	$4(8) \times 10^2$	372(1)
18-C-6[b]	10.2(0.1)	12.7(0.1)	$2.6(0.4) \times 10^5$	$3.8(0.5) \times 10^3$
$\langle N18N\rangle[CH_2$-CO-$N(C_5H_{11})_2]_2$	10.19(0.01)	15.12(0.03)	$1.62(0.03) \times 10^5$	36(2)

[a] The numbers in parentheses are the standard deviations. [b] Detellier's result at 301.5 K.[14a]

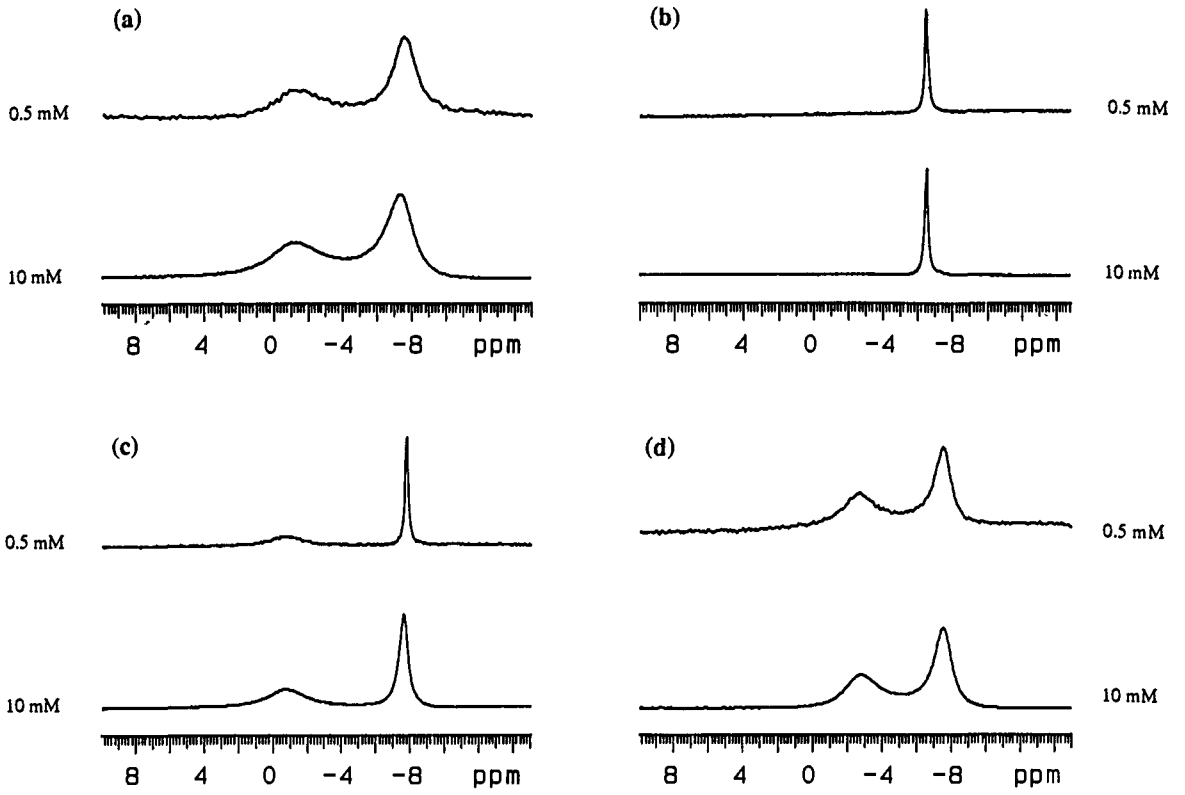

Figure 4. ^{23}Na NMR spectra of $\langle 15N\rangle CH_2$-CO-NHC_5H_{11}/Na^+ (a), 15-C-5/Na^+ (b), $\langle 15N\rangle CH_2$-CO-$N(C_5H_{11})_2/Na^+$ (c), and $\langle 15N\rangle CH_2$-CO-$OC_{10}H_{21}/Na^+$ (d) at total sodium concentrations of 0.5 (top) and 10 mM (bottom) with a 2:1 Na^+/ligand ratio in CD_3CN.

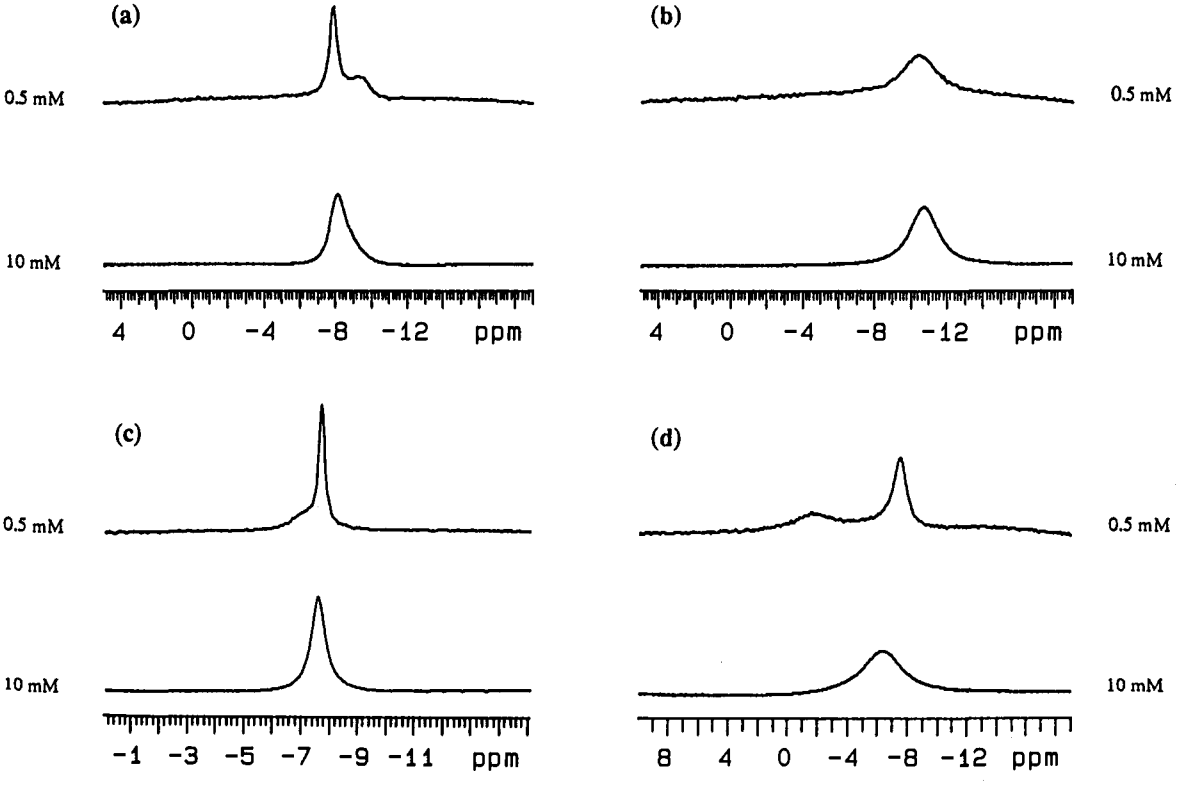

Figure 5. ^{23}Na NMR spectra of $\langle 18N\rangle CH_2$-CO-$OC_{10}H_{21}/Na^+$ (a), 18-C-6/Na^+ (b), $\langle 18N\rangle CH_2$-CO-$N(C_5H_{11})_2/Na^+$ (c), and $\langle 12N\rangle CH_2$-CO-$N(C_5H_{11})_2/Na^+$ (d) at total sodium concentrations of 0.5 (top) and 10 mM (bottom) with a 2:1 Na^+/ligand ratio in CD_3CN.

18-C-6/Na^+ in Table 2 was borrowed from their work.[30] Based on their results and the fact that the total Na^+ concentration used here was half of that used by them in their work,[30] the unimolecular mechanism is probably favored under the present conditions for both of these complexes.

These mechanistic differences are clearly the result of contributions arising both from the macroring size and from the nature of the side arm present. The predominance of the dissociative pathway in both 15-C-5/Na^+ and 18-C-6/Na^+ indicates that ring size is not, by itself, the only factor in the mechanistic choice. Both of these complexes have cations that

(30) (a) Graves, H. P.; Detellier, C. *J. Am. Chem. Soc.* **1988**, *110*, 6019. (b) Briere, K. M.; Detellier, C. *New J. Chem.* **1989**, *13*, 145.
(31) Binsch, G.; Kessler, H. *Angew. Chem., Int. Ed. Engl.* **1980**, *19*, 411.

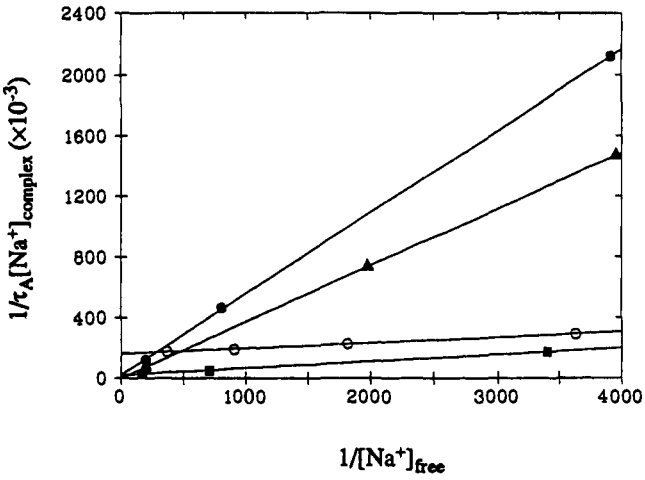

Figure 6. Representative plots of $1/\tau_A[Na^+]_{complex}$ vs $1/[Na^+]_{free}$ for ⟨15N⟩CH_2-CO-NHC_5H_{11}/Na^+ (●), ⟨15N⟩CH_2-CO-$OC_{10}H_{21}/Na^+$ (▲), ⟨15N⟩CH_2-CO-$N(C_5H_{11})_2/Na^+$ (■), and ⟨N18N⟩$[CH_2$-CO-$N(C_5H_{11})_2]_2/Na^+$ (○) in CD_3CN at 21 °C.

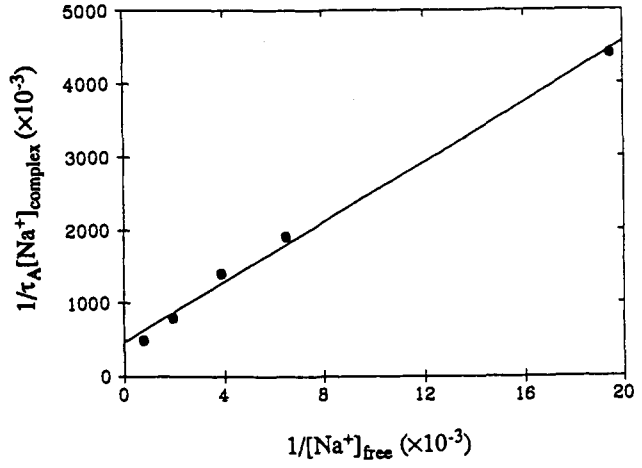

Figure 7. Plot of $1/\tau_A[Na^+]_{complex}$ vs $1/[Na^+]_{free}$ for ⟨12N⟩CH_2-CO-$N(C_5H_{11})_2/Na^+$ in CD_3CN at 21 °C.

are fairly exposed to the solvent medium, since encapsulation of the cation is not possible in either case. Therefore, the unimolecular dissociative pathway is the dominant mechanistic route in both instances.

One striking conclusion that can be derived immediately upon inspection of Table 2 is that both associative and dissociative processes are slowed down when side arms are placed on the macroring. This is evident when comparing the data of 18-C-6/Na^+ with those of all other entries in the table.

Some generalizations can be made on the basis of the ring sizes of these substituted aza-crown ethers. The 18-C-6 derivatives seem to prefer the bimolecular or associative route, while the 15-C-5 derivatives seem to favor the dissociative pathway. The reason why the 18-C-6 derivatives prefer the bimolecular route is probably related to their larger ring size, their consequently larger flexibility, and the presence of a cation-coordinating side arm. Similar observations have been made for dibenzo-24-C-8/Na^+ [15] and dibenzo-30-C-10/Na^+.[16] These large macrocycles are able to bind two cations simultaneously, as evidenced by their X-ray structures, and thus the bimolecular mechanism dominates their exchange properties in some media.[16] The relatively large ring size of the 18-C-6 derivatives, compared with that of the 15-C-5 systems, allows a second Na^+ to approach the already formed complex from the opposite side of where the side arm is interacting with the bound cation. The flexibility of the ring and the larger number of oxygens present (compared with the 15-C-5 derivatives) also favors the interaction with a second approaching cation. At the same time, the strong coordination of the side arm with the bound cation also contributes to the bimolecular process by removing that ion from the macroring as the second cation enters the cavity from the opposite side. This interaction allows the bound cation to exit the complex and to become solvated in discrete stages, while a strong interaction is kept with the ligand via the side-arm donor group. This is only possible for the 18-C-6 derivatives since the macroring cavity size and flexibility both favor the formation of a complex with a second cation approaching from the other side of the side arm. Thus the preferential bimolecular pathway for the 18-C-6 series.

This process is not favored by the smaller and more rigid 15-C-5 ring. Although the side-arm binding argument used above for the 18-C-6 derivatives should apply equally well for the 15-C-5 systems, the smaller ring size in the latter does not lead to a favorable binding nor to a convenient entrance port for the second cation. Therefore, the bimolecular process is not very favorable. This is clearly evident from the values in Table 2, where k_2 values are lower for the 15-C-5 series. It is possible that the bimolecular mechanism in the 15-C-5 series, which does occur to a relatively small extent, involves the simultaneous binding of two Na^+ which are on the same side of the macrocycle in the transition state. The flexibility of the side arm and its motion due to its nitrogen pivot position on the macroring can result in an open structure where it is conceivable that two Na^+ could be bound simultaneously.

One point must be stressed related to the mechanistic behavior of the 15-C-5 series. Although it is true that the bimolecular process is disfavored and that the dissociative pathway is preferred, neither one is particularly efficient. Another way of stating this is to say that the 15-C-5 derivative complexes are kinetically relatively inert. For example, notice that one of the lowest k_{-1} values is that of ⟨15N⟩CH_2-CO-$N(C_5H_{11})_2/Na^+$, while its k_2 value is also very low, see Table 2. These observations indicate that the three-dimensional fit of the cation in the 15-C-5 derivatives is better than in the 18-C-6 analogues, resulting in complexes where the solvent has hindered accessibility to the cation, a somewhat comparable situation to that of the cryptates.[29] Therefore, the 15-C-5 derivative complexes are kinetically, but not thermodynamically, more stable than the corresponding 18-C-6 analogues.[37]

In the case of ⟨N18N⟩$[CH_2$-CO-$N(C_5H_{11})_2]_2/Na^+$, the bimolecular pathway dominates and the dissociative one is the slowest of all of the systems studied, see Table 2. This observation is entirely consistent with the observations with the other 18-C-6 systems. However, its somewhat extreme behavior is probably the result of its having two strongly binding amide side arms instead of one. It is not important to know the precise orientation of the side arms relative to the macroring (syn or anti) upon complexation with Na^+, since both would facilitate the bimolecular pathway by offering two strong binding sites in the two side arms. This is why the bimolecular rate constant is relatively high while k_{-1} is so low.

The behavior of ⟨12N⟩CH_2-CO-$N(C_5H_{11})_2/Na^+$ is somewhat unique but fits into the model described above. The plot of $1/\tau_A[Na^+]_{complex}$ vs $1/[Na^+]_{free}$ for this complex is presented in Figure 7. Both dissociative and associative mechanistic contributions are apparent from the graph. Of all of the ligands investigated, this is the only one where the cation cannot be encapsulated in a three-dimensional fashion, due to the small size of the macroring. As a consequence, the bound cation is always exposed to the solvent, thus facilitating decomplexation. Such a situation could also lead to the penetration of solvent molecules into the complex, leading to partial decomplexation of the cation by the macroring (or the side arm), thus leaving some binding sites available for a second cation to enter, favoring the bimolecular pathway.

Determination of Kinetic Parameters from Variable Temperature ^{23}Na NMR Spectroscopy. Since limited data were obtained

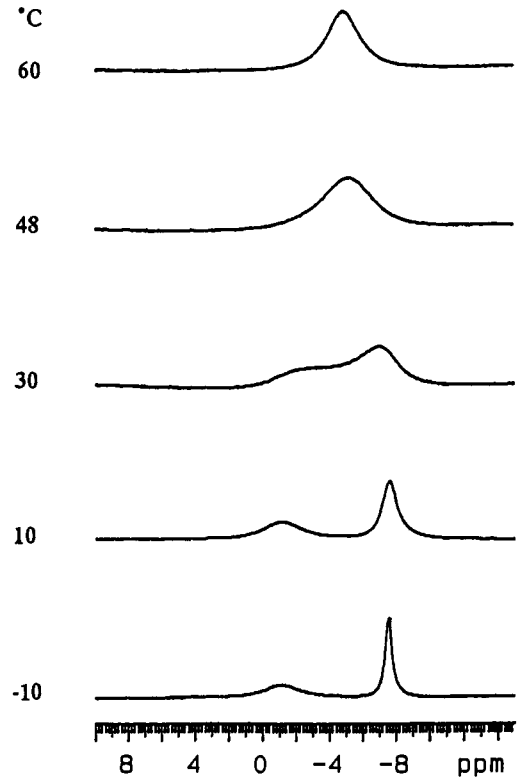

Figure 8. ^{23}Na NMR spectra of $(15N)CH_2$-CO-NHC_5H_{11}/Na^+ with a 2:1 Na^+/ligand ratio at various temperatures.

from the variable concentration studies and since the values of $\Delta H^{\ddagger}$ and $\Delta S^{\ddagger}$ were desired for a deeper understanding of the mechanisms, variable temperature experiments were conducted.

The results of a typical variable temperature experiment are presented in Figure 8 for $(15N)CH_2$-CO-NHC_5H_{11}/Na^+. Eyring plots were constructed for each complex, using at least four or five measurements at different temperatures. Figure 9 shows a typical plot for $(15N)CH_2$-CO-$N(C_5H_{11})_2/Na^+$. All of the activation parameters for the complexes are summarized in Table 3. Also included in the table are the coalescence temperatures (T_C) and the activation free energies at the T_C ($\Delta G^{\ddagger}_C$) for comparison. The activation free energies at the coalescence temperature ($\Delta G^{\ddagger}_C$) can be calculated directly from the value of T_C and the observed line width at half-height using eq 8.[32]

$$\Delta G^{\ddagger}_C = 4.57\ T_C[9.97 + \log(T_C/\delta\nu_{1/2})] \qquad (8)$$

As can be immediately noticed from Table 3, it was not possible to obtain activation parameters for most of the 18-C-6 derivatives.

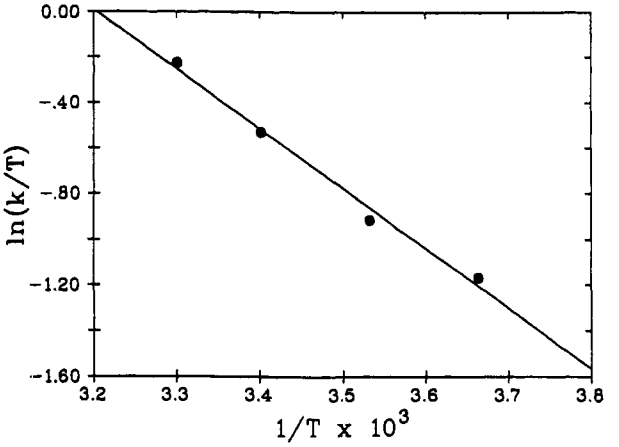

Figure 9. Eyring plot for sodium cation exchange for $(15N)CH_2$-CO-$N(C_5H_{11})_2/Na^+$.

It was only possible for 18-C-6/Na^+, $(N18N)[CH_2$-CO-$N(C_5H_{11})_2]_2/Na^+$, and $(18N)C_3H_6CH{=}CH_2/Na^+$. These were the only 18-C-6 systems that exhibited good base-line separation of the Na^+ resonances. For the other 18-C-6 complexes, the chemical shift differences between the complexed and solvated Na^+ resonances were very small and the former were very broad. It was thus virtually impossible to obtain accurate measurements.

All of the 15-C-5 derivative complexes exhibited a similar activation energy. Even the differences among the enthalpies and the entropies are not particularly significant, although it can be seen that the lower the $\Delta H^{\ddagger}$ value for the decomplexation step, the lower the $\Delta S^{\ddagger}$ becomes. Therefore, there is an enthalpy–entropy compensation effect, although all dissociation processes are both enthalpically and entropically unfavorable. Due to this compensation effect, overall differences in $\Delta G^{\ddagger}_{21\,°C}$ for all of the complexes are very small. It is safe to conclude that such uniformity reflects the similarities of the transition states and the fact that all of the 15-C-5 complexes seem to prefer the unimolecular dissociation pathway. A similar enthalpy–entropy compensation effect of the activation parameters for cation exchange has been recently reported by Detellier and co-workers with some 15-C-5 and 18-C-6 complexes with Na^+.[15b]

It is evident that the length of the lipophilic chains connected to these ligands does not play a major role in their cation-exchange kinetics. It is interesting to note that the $\Delta G^{\ddagger}_{21\,°C}$ values determined for $(15N)CH_2$-CO-NHC_5H_{11}/Na^+ and for $(15N)$-CH_2-CO-$OC_{10}H_{21}/Na^+$ are the same as $\Delta G^{\ddagger}_{21\,°C}{}^{unl}$ determined from the variable concentration experiments described in the previous section. Yet the $\Delta G^{\ddagger}_{21\,°C}$ value for $(15N)CH_2$-CO-$N(C_5H_{11})_2/Na^+$ is lower than the corresponding $\Delta G^{\ddagger}_{21\,°C}{}^{unl}$ determined via the dilution experiments. This may be a reflection

Table 3. Activation Parameters for Sodium Exchange Processes of the Crown Ether Derivative/Na^+ Complexes Measured by ^{23}Na NMR in CD_3CN[a]

compound	$\Delta G^{\ddagger}_{21\,°C}$ (kcal/mol)	$\Delta H^{\ddagger}$ (kcal/mol)	$\Delta S^{\ddagger}$ (cal/mol·K)	$\Delta G^{\ddagger}_c$ (kcal/mol)	T_c (°C)
$(12N)CH_2$-CO-$N(C_5H_{11})_2$	13.2(0.1)	3.8(0.4)	−32(1)	13.5	25
$(15N)CH_2$-CO-$N(C_5H_{11})_2$	14.0(0.1)	5.2(0.4)	−30(1)	>15.6	>70
$(15N)CH_2$-CO-$N(C_{10}H_{21})_2$	13.9(0.1)	5.7(0.3)	−28(1)	>15.6	>70
$(15N)CH_2$-CO-NHC_5H_{11}	13.4(0.1)	6.6(0.5)	−23(2)	14.6	48
$(15N)CH_2$-CO-$NHC_{10}H_{21}$	13.6(0.2)	7.2(0.4)	−22(2)	14.6	48
$(15N)CH_2$-CO-$OC_{10}H_{21}$	13.9(0.1)	6.0(0.4)	−27(1)	14.8	48
$(15N)C_4H_9$	13.4(0.2)	4(1)	−32(4)	12.9	10
15-C-5	[b]	[b]	[b]	11.7	−23
18-C-6	12.7(0.1)	5.1(0.5)	−26(2)	[b]	7
$(18N)C_3H_6CHCH_2$	13.5(0.2)	4.7(0.4)	−30(2)	[b]	12
$(18N)CH_2$-CO-$N(C_5H_{11})_2$	[b]	[b]	[b]	[b]	−5[c]
$(18N)CH_2$-CO-$N(C_{10}H_{21})_2$	[b]	[b]	[b]	[b]	0[c]
$(18N)CH_2$-CO-$NHC_{10}H_{21}$	[b]	[b]	[b]	[b]	−7[c]
$(18N)CH_2$-CO-$NHC_{18}H_{37}$	[b]	[b]	[b]	[b]	−5[c]
$(18N)CH_2$-CO-$OC_{10}H_{21}$	[b]	[b]	[b]	[b]	30[c]
$(N18N)[CH_2$-CO-$N(C_5H_{11})_2]_2$	13.9(0.2)	1.8(0.1)	−41(1)	14.3	43

[a] The numbers in parentheses are the standard deviations. [b] Unable to be measured in the available temperature range. [c] Estimated value.

of a more significant contribution from the less energetic bimolecular exchange pathway to the overall exchange process. Thus the importance of the variable concentration mechanistic work.

Experimental Section

NMR Experiments. Sodium tetraphenylborate (Aldrich, Gold Label) was recrystallized from acetonitrile and vacuum dried at 40 °C for at least 24 h prior to use. 18-Crown-6 and 15-crown-5 (Aldrich) were vacuum dried for at least 12 h prior to use. Acetonitrile-d_3, methanol-d_4, acetone-d_6, and dimethyl sulfoxide-d_6 (Aldrich) were used directly as received.

^{23}Na NMR measurements were carried out using a Varian VXR 400 spectrometer operating at 105.8 MHz. Chemical shifts were referenced to 3 M NaCl aqueous solution without correction for bulk diamagnetic susceptibility differences between the organic solvents and the aqueous reference sample. Sample temperature was controlled by a Varian VXR-400S variable temperature unit to within ±0.5 K. The temperature range was between 233 and 343 K. Sample concentrations were 10 mM for the cation unless otherwise specified. All ^{23}Na NMR spectra were recorded within 24 h after sample preparation. ^{23}Na NMR spectra were acquired with $2K$ data points and zero-filled to $4K$. Line broadening of 1 Hz was used.

A typical sample contained 3 mL of CD_3CN in a 10-mm-i.d. NMR sample tube. The concentration of the ligand was typically 5 mM, and that of Na^+ was always twice the ligand value. Since all of the ligands studied here have relatively high stability constants with Na^+ in CH_3OH,[24] it was reasonable to assume that they would have even larger values in CD_3CN. Therefore, $[Na^+]$ was selected to be twice as large as [L], so that the free ($[Na^+]_{free}$) concentration was approximately equal to that of the complex, $[Na^+] = [(L\text{–}Na^+)]$.

Line widths were measured directly from the line width of the solvated sodium signals at half-height. W_0 was the line width of a 10 mM sodium tetraphenylborate solution in CD_3CN in the absence of cation exchange. Activation enthalpies and entropies were calculated from the Eyring plot by using the program MINSQ. The errors on $\Delta H^\ddagger$ and $\Delta S^\ddagger$ are the standard deviations of the linear regressions of the Eyring plots (Figure 9). Similarly, the errors on k_{-1} and k_2 are the standard deviations of the slope and the intercept from the linear regression of $1/\tau_A[Na^+]_{complex}$ vs $1/[Na^+]_{free}$ (see Figures 6 and 7). The standard deviations for $\Delta G^\ddagger_{21\,°C}$ have been calculated by using the approximate equation $\sigma(\Delta G^\ddagger) = |\sigma(\Delta H^\ddagger) - T\sigma(\Delta S^\ddagger)|$.[31] The errors on $\Delta G^\ddagger_{21\,°C}{}^{uni}$ and $\Delta G^\ddagger_{21\,°C}{}^{bi}$ have been calculated from the corresponding errors of k_{-1} and k_2 at 294 K.[32]

Synthesis. General Information. All chemicals used were purchased from Aldrich Chemicals. Solvents were purified by standard methods. Reactions were performed under an atmosphere of dry N_2 unless otherwise noted. Thin-layer chromatography (TLC) analyses were performed on EM Science aluminum oxide 60 F-254 neutral (type E) with a 0.2-mm layer thickness. Preparative chromatography columns were packed with EM Science activated neutral aluminum oxide (Brockman, 150 mesh, standard grade) unless otherwise noted. The ratios of solvents used for chromatography are given in volumes. Spectra were recorded in $CDCl_3$ on a Varian VXR 400 NMR spectrometer. Chemical shifts are reported in ppm (δ) downfield from internal Me_4Si in the following order: chemical shift, peak multiplicity (br = broad, s = singlet, t = triplet, q = quartet, m = multiplet), integration, coupling constant where applicable, and assignment. Infrared spectra (IR) were recorded on a Perkin-Elmer 1310 spectrophotometer. Spectral bands are reported in cm^{-1} and are calibrated against the 1601-cm^{-1} band of polystyrene. The desorption chemical ionization (DCI) mass spectra (MS) were determined by using ammonia as the reagent gas unless otherwise noted; results were obtained on a VG Trio-2 instrument. Melting points were determined on a Thomas-Hoover 6406-k capillary melting point apparatus in open capillary tubes and are uncorrected. Molecular distillations were performed in a Kugelrohr apparatus (Aldrich), and the distillation temperatures reported refer to its oven temperature. Elemental analyses were conducted by Atlantic Microlab Inc., Atlanta, GA.

General Procedure For The Preparation of the Substituted Crown Ethers. 2-[*N*-(1,4,7-Trioxa-10-azacyclododecyl)]-*N*,*N*-dipentylacetamide, ⟨12N⟩-CH_2-CO-N(C_5H_{11})$_2$. Aza-12-crown-4[33] (1.3 g, 7.4 mmol), 2-chloro-*N*,*N*-dipentylacetamide,[34] (1.73 g, 8.0 mmol), and Na_2CO_3 (1.55 g, 14.8 mmol) were added at once to butyronitrile (50 mL). The resulting mixture was stirred at reflux temperature for 24 h, cooled to room temperature, filtered, and concentrated under reduced pressure to a heavy yellow oil. The resulting yellow oil was redissolved in CH_2Cl_2 (100 mL) and washed with 3 N HCl (3 × 30 mL), 5% Na_2CO_3 (3 × 30 mL), and brine (30 mL), dried over $MgSO_4$, and concentrated under reduced pressure. The residue was chromatographed on alumina, neutral (0–2% (v/v) MeOH/CH_2Cl_2), to give a pale yellow oil that afforded the desired compound as a colorless heavy oil after bulb-to-bulb distillation in 75% yield [bp 150–152 °C (0.15 Torr)]: ^{1}H NMR δ 0.90 (m, 6H, CH_3), 1.27 (m, 8H, CH_2), 1.52 (m, 4H, N-C-CH_2), 2.94 (t, 4H, J = 4.6 Hz, [O-C-CH_2]$_2$-N), 3.26 (m, 4H, CO-N-CH_2), 3.49 (s, 2H, N-CH_2-CO), 3.61 (t, 4H, J = 4.6 Hz, [O-CH_2-C]$_2$N), 3.68 (m, 8H, crown); IR (neat) 2880 (s), 1620 (s), 1430 (s) cm^{-1}; DCI mass spectrum m/z (relative intensity) 374 (23, MH^+), 373 (100, M^+). Anal. Calcd for $C_{20}H_{40}N_2O_4$: C, 64.48; H, 10.82. Found: C, 64.23; H, 10.84.

2-[*N*-(1,4,7,10-Tetraoxa-13-azacyclopentadecyl)]-*N*,*N*-dipentylacetamide, ⟨15N⟩CH_2-CO-N(C_5H_{11})$_2$. The compound was obtained from aza-15-crown-5[35] and 2-chloro-*N*,*N*-dipentylacetamide as a colorless oil in 70% yield after column chromatography on alumina, neutral (0–10% (v/v) 2-propanol/hexanes), followed by reduced-pressure distillation [bp 170–172 °C (0.15 Torr)]: ^{1}H NMR δ 0.90 (t, 6H, J = 6.6 Hz, CH_3), 1.32 (m, 8H, CH_2), 1.55 (m, 4H, N-C-CH_2), 2.73 (t, 4H, J = 5.0 Hz, [O-C-CH_2]$_2$N), 3.16 (s, 2H, CO-CH_2-N), 3.25 (m, 2H, N-CH_2-C), 3.54 (t, 4H, J = 5.0 Hz, [O-CH_2-C]$_2$N), 3.67 (m, 12H, crown), 8.03 (br, 1H, NH); IR (CCl_4) 3350 (m), 2940 (s), 2880 (s), 1660 (s), 1520 (m) cm^{-1}; DCI mass spectrum m/z (relative intensity) 348 (25, MH^+), 347 (100, M^+). Anal. Calcd for $C_{17}H_{34}N_2O_5$1/2H_2O: C, 57.44; H, 9.92. Found: C, 57.67; H, 9.94.

2-[*N*-(1,4,7,10-Tetraoxa-13-azacyclopentadecyl)]-*N*,*N*-didecylacetamide, ⟨15N⟩CH_2-CO-N($C_{10}H_{21}$)$_2$. The crude compound was obtained from aza-15-crown-5 and 2-chloro-*N*,*N*-didecylacetamide as a light yellow oil after two consecutive column chromatographies on alumina, neutral (0–0.5% (v/v) MeOH/CH_2Cl_2 followed by 1–5% (v/v) 2-propanol/hexanes). The crude light yellow oil afforded the pure compound as a colorless oil in 71% yield after reduced pressure distillation [bp 185–188 °C (0.15 Torr)]: ^{1}H NMR δ 0.88 (m, 6H, CH_3), 1.26 (br, 28H, CH_2), 1.51 (m, 4H, N-C-CH_2), 2.92 (t, 4H, J = 5.8 Hz, [O-C-CH_2]$_2$N), 3.26 (t, 4H, J = 7.9 Hz, N-CH_2-C), 3.44 (s, 2H, CO-CH_2-N), 3.66 (m, 16H, crown); IR (neat) 2920 (s), 2880 (s), 1630 (s), 1445 (s) cm^{-1}; DCI mass spectrum m/z (relative intensity) 558 (25, MH^+), 557 (M^+). Anal. Calcd for $C_{32}H_{64}N_2O_5$: C, 69.02; H, 11.58. Found: C, 68.85; H, 11.55.

2-[*N*-(1,4,7,10-Tetraoxa-13-azacyclopentadecyl)]-*N*-pentylacetamide, ⟨15N⟩CH_2-CO-NHC_5H_{11}. The compound was obtained from aza-15-crown-5 and 2-chloro-*N*-pentylacetamide as a colorless heavy oil in 72% yield after purification by column chromatography on alumina, neutral (0–2% (v/v) MeOH/CH_2Cl_2), followed by a second column chromatography on alumina, neutral (0–10% (v/v) 2-propanol/hexanes), and finally reduced-pressure distillation [bp 158–160 °C (0.15 Torr)]: ^{1}H NMR δ 0.90 (t, 3H, CH_3), 1.28 (m, 4H, CH_2), 1.52 (m, 2H, N-C-CH_2), 2.92 (t, 4H, J = 5.8 Hz, [O-C-CH_2]$_2$N), 3.26 (t, 4H, J = 6.5 Hz, N-CH_2-C), 3.45 (s, 2H, CO-CH_2N), 3.66 (m, 16H, crown); IR (neat) 2920 (s), 2840 (s), 1630 (s), 1440 (s) cm^{-1}; DCI mass spectrum m/z (relative intensity) 418 (20, MH^+), 417 (100, M^+). Anal. Calcd for $C_{22}H_{44}N_2O_5$: C, 63.43; H, 10.65. Found: C, 63.29; H, 10.66.

2-[*N*-(1,4,7,10-Tetraoxa-13-azacyclopentadecyl)]-*N*-decylacetamide, ⟨15N⟩CH_2-CO-NH$C_{10}H_{21}$. The compound was obtained from aza-15-crown-5 and 2-chloro-*N*-decylacetamide as a yellow oil in 76% yield after purification by column chromatography on alumina, neutral (0–5% (v/v) 2-propanol/hexanes): ^{1}H NMR δ 0.88 (m, 3H, CH_3), 1.26 and 1.29 (br, 14H, CH_2), 1.53 (m, 2H, N-C-CH_2), 2.72 (m, 4H, [O-C-CH_2]$_2$N), 3.15 (s, 2H, CO-CH_2-N), 3.23 (m, 2H, N-CH_2-C), 3.53 (m, 4H, [O-CH_2-C]$_2$N), 3.61 and 3.65 (m, 12H, crown) 8.02 (s, 1H, NH); IR (neat) 3310 (m), 2920 (s), 2840 (s), 1650 (s), 1520 (m) cm^{-1}; DCI mass spectrum m/z (relative intensity) 418 (20, MH^+), 417 (100, M^+). Anal. Calcd for $C_{22}H_{44}N_2O_5$: C, 63.43; H, 10.65. Found: C, 63.25; H, 10.69.

2-[*N*-(1,4,7,10,13-Pentaoxa-16-azacyclooctadecyl)]-*N*,*N*-dipentylacetamide, ⟨18N⟩CH_2-CO-N(C_5H_{11})$_2$. The crude compound was obtained from aza-18-crown-6[35] and 2-chloro-*N*,*N*-dipentylacetamide as a light yellow oil after several consecutive column chromatography purifications

(32) Ref 22, p 109.
(33) Calverley, M. J.; Dale, J. *Acta Chem. Scand. B* **1982**, *36*, 241.
(34) Gokel, G. W.; Hernández, J. C.; Viscariello, A. M.; Arnold, K. A.; Campana, C. F.; Fronczek, F. R.; Gandour, R. D.; Morgan, C. R.; Trafton, J. E.; Miller, S. R.; Minganti, C.; Eiband, D.; Schultz, R. A.; Tamminen, M. *J. Org. Chem.* **1987**, *52*, 2963.

on alumina (neutral) using the following solvent mixtures respectively: 0–2% (v/v) MeOH/CH_2Cl_2, 0–5% (v/v) 2-propanol/hexanes, 1:49.5:49.5 (in volume) MeOH/hexanes/CH_2Cl_2. The crude light yellow oil was then distilled in a Kugelrohr apparatus to afford the pure compound as a colorless oil in 55% yield [bp 185–187 °C (0.15 Torr): ^{1}H NMR δ 0.90 (m, 6H, CH_3), 1.31 (m, 8H, CH_2), 1.52 (m, 4H, N-C-CH_2), 2.92 (t, 4H, J = 5.8 Hz, [O-C-CH_2]$_2$N), 3.28 (m, 4H, N-CH_2-C), 3.45 (s, 2H, CO-CH_2-N), 3.56 (m, 20H, crown); IR (neat) 2900 (s), 1630 (s), 1440 (s) cm^{-1}; DCI mass spectrum m/z (relative intensity) 462 (25, MH^+), 461 (100, M^+). Anal. Calcd for $C_{24}H_{48}N_2O_6$: C, 62.58; H, 10.50. Found: C, 62.61; H,1 0.56.

2-[*N*-(1,4,7,10,13-Pentaoxa-16-azacyclooctadecyl)]-*N*,*N*-didecylacetamide, ⟨18N⟩CH_2-CO-N($C_{10}H_{21}$)$_2$. The pure compound was obtained from aza-18-crown-6 and 2-chloro-*N*,*N*-didecylacetamide as a light yellow oil in 61% after purification by column chromatography on alumina, neutral (0–5% (v/v) 2-propanol/hexanes). No distillation was attempted: ^{1}H NMR δ 0.88 (m, 6H, CH_3), 1.27 (br, 28H, CH_2), 1.51 (m, 4H, N-C-CH_2), 2.94 (br, 4H, [O-C-CH_2]$_2$N), 3.27 (m, 4H, N-CH_2-C), 3.45 (s, 2H, CO-CH_2-N), 3.67 (m, 20H, crown); IR (CCl_4) 2940 (s), 2860 (s), 1640 (m), 1460 (m) cm^{-1}; DCI mass spectrum m/z (relative intensity) 602 (35, MH^+), 601 (100, M^+). Anal. Calcd for $C_{34}H_{68}N_2O_6$: C, 67.96; H, 11.41. Found: C, 67.74; H, 11.47.

2-[*N*-(1,4,7,10,13-Pentaoxa-16-azacyclooctadecyl)]-*N*-octadecylacetamide, ⟨18N⟩CH_2-CO-N$HC_{18}H_{37}$. The compound was obtained from aza-18-crown-6 and 2-chloro-*N*-octadecylacetamide as a white solid (mp 27–28 °C) in 60% yield after purification by column chromatography on alumina, neutral (0–5% (v/v) 2-propanol/hexanes), followed by recrystallization from hexanes: ^{1}H NMR δ 0.88 (t, 3H, J = 6.8 Hz, CH_3), 1.25 (br, 30H, CH_2), 1.52 (m, 2H, N-C-CH_2), 2.75 (t, 4H, J = 5.2 Hz, [O-C-CH_2]$_2$N), 3.17 (s, 2H, CO-CH_2-N), 3.24 (q, 2H, J_{ab} = 6.6 Hz, J_{bc} = 6.4 Hz, N-CH_2-C), 3.56 (t, 4H, J = 5.2 Hz, [O-CH_2-C]$_2$N), 3.64 (m, 16H, crown), 7.86 (s, 1H, NH); IR (KBr) 3420 (s), 2920 (s), 2860 (s), 1640 (m), 1450 (w) cm^{-1}; DCI mass spectrum m/z (relative intensity) 573 (100, M^+). Anal. Calcd for $C_{32}H_{64}N_2O_6$: C, 67.09; H, 11.26. Found: C, 67.03; H, 11.21.

Decyl[*N*-(1,4,7,10-Tetraoxa-13-azacyclopentadecyl)]acetate, ⟨15N⟩-CH_2-CO-$OC_{10}H_{21}$. The compound was obtained from aza-15-crown-5 and decyl chloroacetate as a yellow oil in 70% yield after purification on alumina, neutral (0–10% (v/v) 2-propanol/hexanes). Reduced pressure distillation indicated that the product decomposes at 95 °C (0.15 Torr). ^{1}H NMR: 0.88 (t, 3H, J = 6.8 Hz, CH_3), 1.26 and 1.30 (br, 14H, CH_2), 1.62 (t, 2H, J = 7.0 Hz, O-C-CH_2), 2.94 (t, 4H, J = 5.8 Hz, [O-C-CH_2]$_2$N), 3.48 (s, 2H, CO-CH_2-N), 3.66 (m, 16H, crown), 4.08 ppm (t, 2H, J = 6.0 Hz, O-CH_2-C). IR (neat): 2920 (s), 2750 (s), 1740 (s), 1440 (m) cm^{-1}. Anal. Calcd for $C_{22}H_{43}NO_6$: C, 63.28; H, 10.38. Found: C, 63.13; H, 10.41. DCI mass spectrum: m/z (relative intensity) 419 (18, MH^+), 418 (100, M^+).

Decyl[*N*-(1,4,7,10,13-Pentaoxa-16-azacyclooctadecane)]acetate, ⟨18N⟩-CH_2-CO-$OC_{10}H_{21}$. The compound was obtained from aza-18-crown-6 and decyl chloroacetate in 62% yield as a pure light yellow oil after purification by two consecutive column chromatographies on alumina (neutral) using the following solvent systems: 0–2% (v/v) MeOH/CH_2Cl_2 and 0–5% (v/v) 2-propanol/hexanes. Distillation was not performed: ^{1}H NMR δ 0.88 (t, 3H, J = 7.0 Hz, CH_3), 1.26 (br, 14H, CH_2), 1.62 (m, 2H, O-C-CH_2), 2.96 (t, 4H, J = 5.5 Hz, [O-C-CH_2]$_2$N), 3.52 (s, 2H, CO-CH_2-N), 3.66 (m, 20H, crown), 4.08 (t, 2H, J = 6.8 Hz, O-CH_2-C); IR (neat) 2920 (s), 2880 (s), 1735 (s), 1455 (s) cm^{-1}; DCI mass spectrum m/z (relative intensity) 463 (22, MH^+), 462 (100, M^+). Anal. Calcd for $C_{24}H_{47}NO_7$: C, 62.44; H, 10.26. Found: C, 62.71; H, 10.39.

Synthesis of 2,2′-[*N*,*N*′-(1,4,10,13-Tetraoxa-7,16-diazacyclooctadecyl)]bis-*N*,*N*-dipentylacetamide, ⟨N18N⟩[CH_2-CO-N(C_5H_{11})$_2$]$_2$. Butyronitrile was substituted by acetonitrile in the preparation of this compound. The title compound was obtained from diaza-18-crown-6[36] as a light yellow oil after usual purification by column chromatography on alumina, neutral (0–5% (v/v) 2-propanol/hexanes), followed by a second column chromatography on alumina, neutral (1:49.5:49.5 (in volume) 2-propanol:hexanes:CH_2Cl_2). No distillation was attempted: ^{1}H NMR δ 0.90 (m, 12H, CH_3), 1.29 (m, 16H, CH_2), 1.51 (m, 8H, N-C-CH_2), 2.93 (t, 8H, J = 5.2 Hz, [O-C-CH_2]$_2$N), 3.27 (m, 8H, N-CH_2-C), 3.45 (s, 4H, CO-CH_2-N), 3.61 (m, 16H, crown); IR (CCl_4) 2940 (s), 2860 (s), 1630 (s), 1450 (s) cm^{-1}; DCI mass spectrum m/z (relative intensity) 658 (48, MH^+), 657 (100, M^+), 472 (45).

Acknowledgment. The authors express their gratitude to the NIH (Grant GM-33940) and the NSF (Grant DMR-9119986) for partial support of this work.

(35) Maeda, H.; Furuyoshi, S.; Nakatsuji, Y.; Okahara, M. *Bull. Chem. Soc. Jpn.* **1983**, *56*, 212.

(36) Gatto, V. J.; Gokel, G. W. *J. Am. Chem. Soc.* **1984**, *106*, 8240.

(37) Note: We have recently observed very similar behavior for the ⟨15N⟩-CH_2-CO-N(C_5H_{11})$_2$/Li^+ complex in a preliminary study conducted using ^{7}Li NMR under similar experimental conditions. $LiClO_4$ (Aldrich) was used as the lithium salt at a concentration of 10 mM and a 2:1 cation/ligand ratio. At room temperature, only one time-averaged Li^+ resonance was observed for both ⟨12N⟩CH_2-CO-N(C_5H_{11})$_2$/Li^+ and ⟨18N⟩CH_2-CO-N(C_5H_{11})$_2$/Li^+, at 1.90 and 1.95 ppm, respectively, while the ⟨15N⟩CH_2-CO-N(C_5H_{11})$_2$/Li^+ complex exhibited two well-separated Li^+ resonances, at –0.02 (δ_c) and –2.22 (δ_f) ppm. This separation is even larger than that observed for [2.1.1]/Li^+ measured under the same experimental conditions, i.e., –0.40 (δ_c) and –2.35 (δ_f) ppm.